Superconductivity in metal-mixed ion-implanted polymer films

A. P. Micolich, E. Tavenner, B. J. Powell, A. R. Hamilton, M. T. Curry, R. E. Giedd, and P. Meredith

Articles you may be interested in

Preparation of metal mixed plastic superconductors: Electrical properties of tin-antimony thin films on plastic substrates
J. Appl. Phys. **105**, 093909 (2009); 10.1063/1.3123803

Conducting Ni nanoparticles in an ion-modified polymer
J. Appl. Phys. **98**, 066101 (2005); 10.1063/1.2014938

Superconductivity suppression in Fe-implanted thin Al films
J. Appl. Phys. **98**, 016105 (2005); 10.1063/1.1946205

Buried superconducting layers comprised of magnesium diboride nanocrystals formed by ion implantation
Appl. Phys. Lett. **80**, 4786 (2002); 10.1063/1.1488695

Effect of implanted metal impurities on superconducting tungsten films
J. Appl. Phys. **91**, 6516 (2002); 10.1063/1.1469690

Superconductivity in metal-mixed ion-implanted polymer films

A. P. Micolich[a)]
School of Physics, University of New South Wales, Sydney NSW 2052, Australia

E. Tavenner and B. J. Powell
Physics Department, University of Queensland, Brisbane QLD 4072, Australia

A. R. Hamilton
School of Physics, University of New South Wales, Sydney NSW 2052, Australia

M. T. Curry and R. E. Giedd
Center for Applied Science and Engineering, Missouri State University, Springfield, Missouri 65804

P. Meredith[b)]
Physics Department, University of Queensland, Brisbane QLD 4072, Australia

Ion implantation of normally insulating polymers offers an alternative to depositing conjugated organics onto plastic films to make electronic circuits. We used a 50 keV nitrogen ion beam to mix a thin 10 nm Sn/Sb alloy film into the subsurface of polyetheretherketone and report the low temperature properties of this material. We observed metallic behavior, and the onset of superconductivity below 3 K. There are strong indications that the superconductivity does not result from a residual thin film of alloy, but instead from a network of alloy grains coupled via a weakly conducting, ion-beam carbonized polymer matrix. © *2006 American Institute of Physics.*
[DOI: 10.1063/1.2358190]

Since the discovery of electrical conductivity in conjugated polymers,[1] intense international effort has focused on the development of electronic devices and integrated circuits on plastic films.[2] 'Plastic electronics' promise significant advantages over existing technologies, including simpler and more efficient processing, mechanical flexibility/robustness, and the possibility of large area ($\sim m^2$) production.[2] Conducting polymers such as heavily doped polyacetylene can exhibit a metallic state.[3,4] However, metallic behavior in organic polymers is not common, and the underlying physics is not well understood.[5] Ion implantation of normally insulating polymers offers an alternative to depositing metals or conjugated organics onto plastic films to make electronic circuits. Further, ion implantation techniques are widely used in the semiconductor industry and could be adapted for processing electronic circuits based on plastic substrates.

Previous studies have reported increased electrical conductivity due to carbonization of the polymer by the ion beam.[6,7] However, despite showing conductivities up to $\sim$300 S/cm, these materials are insulators, exhibiting increasing resistivity with decreasing temperature. Achieving metallic conductivity in ion-implanted polymers is a longstanding problem. Recently, implantation of polyetheretherketone [PEEK – chemical structure shown in inset to Fig. 1(c)] using a metallic Sn ion beam was explored.[8] However, this resulted in a maximally implanted ion content insufficient for metallic conductivity due to a self-limiting sputtering process. One way to overcome this problem is to deposit a thin metal layer on the polymer substrate and then use an ion beam to "mix" this metal into the polymer subsurface—a process known as "metal mixing."[9] The rationale behind metal mixing is that lower mass inert ions can be used, re-

ducing the sputtering, while the metal layer ensures that after implantation, sufficient metal atoms have been mixed into the polymer to allow metallic conductivity.

In this letter, we present a low-temperature electrical study of this Sn:Sb/PEEK metal mixed system. In addition to a weak metallic temperature dependence, we observe the
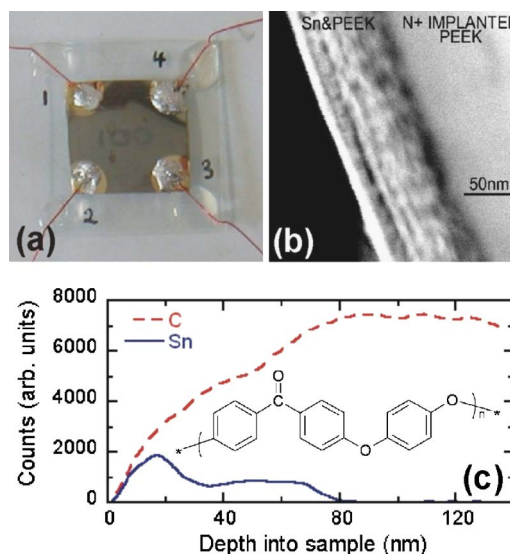

FIG. 1. (Color online) A photograph of a metal-mixed sample which consists of a 10 nm layer of Sn:Sb alloy on a 0.1-mm-thick PEEK film that was subsequently implanted with a 50 keV N+ beam to a dose of 10^{16} ions/cm^2. The sample is 15 mm square with 50 nm Ti/50 nm Au contacts evaporated in the corners and wires attached using InAg solder. (b) Cross-sectional STEM image of a metal mixed sample, and (c) corresponding energy dispersive x-ray analysis (EDAX) profile showing the relative concentrations of Sn (solid line) and C (dashed line) in the near surface of the PEEK; (b) and (c) demonstrate that implantation has mixed the initial 10 nm Sn:Sb alloy layer over $\sim$75 nm of the subsurface region of the PEEK film. The chemical structure of PEEK is inset to (c).

a)Electronic mail: mico@phys.unsw.edu.au
b)Electronic mail: meredith@physics.uq.edu.au

onset of superconductivity at temperatures $T < 3$ K. Previous studies of organic superconductor-polymer blends (e.g., β'-(ET)$_2$I$_3$ microcrystals in polycarbonate) have observed a partial Meissner effect.[10] Here we report a plastic material that shows a complete transition to a robust zero electrical resistance state, suggesting potential technological applications for the ion-beam processed polymer that are not possible with superconducting-polymer blends.

Our samples were prepared by evaporating a $\sim$10 mm layer of 95% Sn: 5% Sb alloy onto a 0.1-mm-thick PEEK film, and implanting the metallized surface to doses of 10^{16} (sample A) and 10^{15} (sample B) ions/cm^2 with a 50 keV N$^+$ beam.[11] We also prepared a control sample consisting of bare PEEK implanted with 50 keV N$^+$ ions to 10^{16} ions/cm^2 (sample C). The 5% Sb plays an essential role in the conductivity of samples A and B. Samples prepared with 100% Sn are strongly insulating, even with Sn film thicknesses as high as 40 nm. The addition of Sb to Sn inhibits its transformation from metallic white allotrope to the insulating gray allotrope.[12] However, it is not yet clear if/how the 5% Sb fraction affects the postimplant structure of the samples – we note that an underlayer of Sb is often used in quench condensed film studies to control the length scale of disorder.[13]

To demonstrate that the ion-beam thoroughly mixes the Sn/Sb alloy film into the PEEK surface, in Fig. 1(b) we show a cross-sectional scanning transmission electron microscopy (STEM) image of the near-surface region of a sample nominally identical to sample A. Clear structural differences are evident between the implant-mixed region extending $\sim$75 nm into the sample, and the bulk polymer. The accompanying elemental analysis, shown in Fig. 1(c), confirms that the original 10 nm of alloy is distributed over more than seven times its original volume. Previous x-ray photoelectron spectroscopy (XPS) studies of this material[8] show that implantation induces three key chemical changes relative to an unimplanted sample: (a) the number of Sn–Sn bonds is reduced by a factor of 4 while the Sn–C bond content is increased from <0.1 to $\sim$5%; (b) there is a net decrease in Sn–Sn bond content in the first $\sim$8.5 nm (the region probed by XPS) of the sample, due to a combination of mixing the Sn deeper into the sample and sputtering by the incident energetic N$^+$ ions, and; (c) the graphitic carbon content is increased from <0.1 to $\sim$27%, consistent with previous studies.[6,7] The XPS data also indicate that much of the 5% Sb fraction is oxidized during implantation, with net Sb loss due to sputtering.[8] Combined, these chemical and structural findings strongly suggest that the alloy film has been thoroughly mixed into the PEEK.

After implantation, the samples were prepared for electrical characterization.[11] Four 5-mm diameter contacts were deposited at the corners of the 15-mm-square samples, to form a quasi-Van der Pauw measurement configuration [see Fig. 1(a)]. Contacts consisting of 50 nm Ti/ 50 nm Au were deposited by thermal evaporation through a shadow mask. After contact deposition, the samples were mounted on 25-mm-square glass slides and insulated Cu wires were attached using low melting point InAg solder.

Electrical measurements were performed in an Oxford Instruments VTI system, which allowed temperatures T between 1.2 and 200 K and magnetic fields B up to 10 T. The d.c. electrical resistance R of the samples was measured using a Keithley 2400 Source-Measure Unit in both two- and four-terminal modes. We commenced by measuring the two-
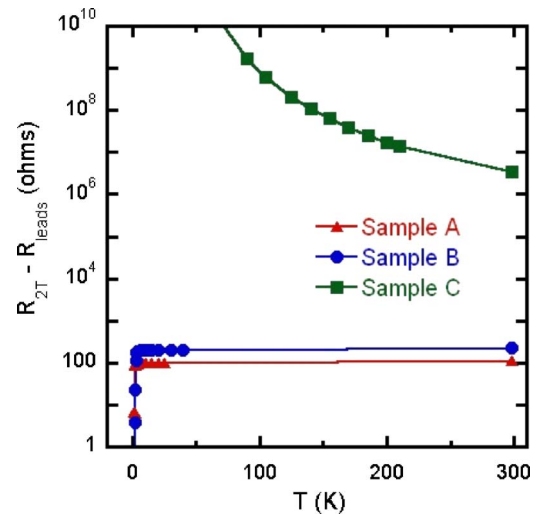

FIG. 2. (Color online) Resistance (two-terminal minus temperature-dependent lead resistance) R_{2T}-R_{leads} vs temperature T for sample A (10 nm Sn:Sb on PEEK, 10^{16} ions/cm^2 50 keV N$^+$), sample B (10 nm Sn:Sb on PEEK, 10^{15} ions/cm^2 50 keV N$^+$) and sample C (bare PEEK, 10^{16} ions/cm^2 50 keV N$^+$). The addition of the thin Sn:Sb layer prior to implantation leads to a metallic temperature dependence in contrast to sample C, which show an insulating temperature dependence. A sharp drop in resistance is apparent in samples A and B at low T.

terminal electrical resistance R_{2T} vs T for the three samples. In order to establish the true T-dependence of the sample, we obtained the temperature dependent lead resistance R_{leads} by simultaneously measuring two identical leads shorted together at the bottom of the cryostat, and subtracted this from R_{2T} to give the data shown in Fig. 2.

Two features are evident in Fig. 2. First, we observe a weak metallic T-dependence in the metal-mixed samples A and B. This is in contrast to sample C, where we observe very strong insulating behavior consistent with previous studies.[6,7] Second, samples A and B, although metallic, are highly disordered. The level of disorder is characterized by the residual resistance ratio (RRR) defined as $\rho(300 \text{ K})/\rho(T_c^+)$, where T_c^+ is a temperature slightly above the critical temperature T_c, and for samples A and B we find a RRR <1.2, indicative of a highly disordered material.

Figure 2 shows a very sharp drop in the resistance at $T < 3$ K. We used four-terminal measurements (Fig. 3) to further explore the possibility of superconductivity. We again observe a clear metallic temperature dependence that culminates in a sharp drop, this time to a zero resistance state ($R_{4T} < 0.01$ Ω, our instrument sensitivity limit) with T_c of 1.9 and 2.4 K for samples A and B, respectively. The observed electrical behavior is repeatable after thermal cycling to room T, and reproducible (quantitatively similar) in nominally identical samples. We also find that the metal-mixed layer does not delaminate even after several cryogenic cycles. We have repeated our measurements over seven months with little change of the electronic properties beyond a slight ($<10\%$) increase in the normal resistance over this period, despite simply storing these samples in a plastic box under ambient conditions. We have also obtained magnetic field dependence measurements on sample A (field perpendicular to plane of the sample) to establish the critical magnetic field B_c. As shown in Fig. 3 (inset), we see a field-induced superconducting-normal transition at $B_c = 0.12$ T,
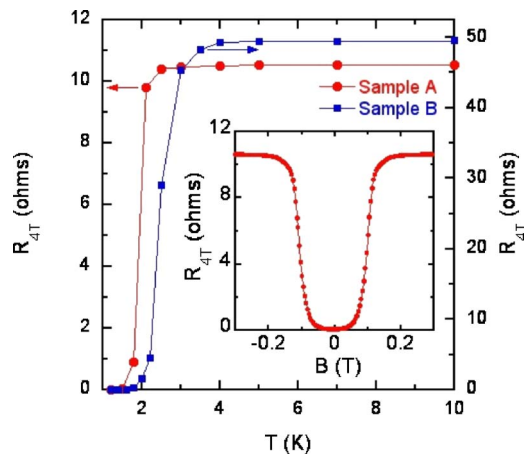
FIG. 3. (Color online) Four-terminal resistance R_{4T} vs T for sample A (left axis) and B (right axis) demonstrating the presence of a zero resistance state at low T. The critical temperatures T_c are 1.9 and 2.4 K for samples A and B, respectively, (inset) R_{4T} vs magnetic field B, oriented perpendicular to the plane of the plastic film, at $T=1.2$ K for sample A, demonstrating a field-induced transition to a normal state. The measured critical field B_c is 0.12 T.

and, as expected, B_c decreases with increasing T. The typical critical current I_c is of order 1 mA.

At first sight, the observation of superconductivity in these samples may not be surprising—Sn is an elemental superconductor with $T_c=3.7$ K and $B_c=30$ mT, and Sb becomes superconducting under pressure. We find that a 20-nm-thick film of Sn:Sb on PEEK (unimplanted) shows a very sharp transition with $T_c=3.7$ K and $B_c\sim 300$ mT (i.e., neither the Sb impurities nor geometrical effects reduce T_c). While the increased B_c is expected due to the thin film geometry, the suppressed T_c observed in samples A and B is surprising if the observed superconductivity results from bulk alloy. Hence we instead consider two models for the superconductivity: (a) a residual layer of alloy thin enough to not only increase B_c, but also suppress T_c, and; (b) a granular alloy system where the weakly conducting ion-beam modified PEEK matrix acts as a weak link between Josephson- or proximity-effect coupled grains. We also note a more exotic possibility (not considered further here): a metal-carbon "eutectic" where the Sn and C are mixed at the molecular level and the Sn acts mainly by doping the hydrocarbon.

We now critically assess the two models against the experimental data. First, the correct model must explain why T_c is significantly suppressed. The suppression of T_c has previously been observed in quench-condensed films grown at low temperatures[13] (≤ 4 K), where higher disorder [indicated by a higher normal resistance $R(T_c^+)$] leads to reduced T_c. Considering the data in Fig. 3 from this viewpoint, we would expect that a lower implant dose would lead to less disorder and consequently a lower $R(T_c^+)$. However, the lower dose sample B actually has a $R(T_c^+)\sim 4$ times higher than sample A. The measured relationships between the $R(T_c^+)$ and T_c values clearly contradict the behavior expected for a residual 2D thin film – *sample A, which has the lower $R(T_c^+)$, and thus the least disorder, actually has the lower T_c.* Furthermore, T_c suppression in quench condensed films only occurs when the resistance is of order the quantum of resistance for electron pairs (i.e., $R(T_c^+)\sim h/4e^2\sim 6450$ $\Omega/\square$), which is more than two orders of magnitude larger than $R(T_c^+)$ in either sample A or B, which were measured in the standard square geometry.

We now consider a network of Sn:Sb alloy granules coupled via a weakly conducting, carbonized polymeric matrix. First, this possibility is consistent with our structural analysis, in particular, the decrease in Sn–Sn bonds and the increase in Sn–C bonds indicated by XPS. The granular model also explains why both the $R(T_c^+)$ and T_c of sample A, which has the higher implant dose, are lower than those of sample B. Considering $R(T_c^+)$ first, in the normal phase, R is dominated by inter-grain hopping and increases with the grain separation. Sample A, which has the higher implant dose, would be expected to contain smaller alloy grains with a smaller inter-grain separation (i.e., better mixing), and hence should have a lower $R(T_c^+)$, as observed in Fig. 3. Considering T_c, supposing that the grains are small enough that they do undergo T_c suppression, then smaller grains would be expected to have a lower T_c, and hence the higher dose sample A would have the lower T_c, as also observed in the data in Fig. 3. While we currently believe that the granular hypothesis gives the most natural explanation for our data, experiments that establish the micro/nano-scale structure of the ion-beam mixed region are required to confirm this hypothesis. We also plan to explore metal mixing of other elements (e.g., Nb) with the goal of increasing T_c.

In conclusion, we have used ion implantation to mix a thin Sn:Sb alloy layer into a PEEK surface to significantly enhance the conductivity. We observe metallic behavior, with superconductivity at $T<3$ K. Our structural and electrical data suggest that the metallic conductivity and superconductivity arise from a network of alloy grains coupled through a weakly conducting, ion-beam carbonized, polymer matrix, as opposed to a residual thin film of alloy.

[1] C. K. Chaing, C. R. Fischer, Y. W. Park, A. J. Heeger, H. Shirakawa, E. J. Louis, S. C. Gau, and A. G. MacDiarmid, Phys. Rev. Lett. **39**, 1098 (1977).
[2] D. Voss, Nature (London) **407**, 442 (2000).
[3] T. Ishiguro, H. Kaneko, Y. Nogami, H. Ishimoto, H. Nishiyama, J. Tsukamoto, A. Takahashi, M. Yamaura, T. Hagiwara, and K. Sato, Phys. Rev. Lett. **69**, 660 (1992).
[4] R. S. Kohlman, A. Zibold, D. B. Tanner, G. G. Ihas, T. Ishiguro, Y. G. Min, A. G. MacDiarmid, and A. J. Epstein, Phys. Rev. Lett. **78**, 3915 (1997).
[5] R. S. Kohlman and A. J. Epstein, in *Handbook of Conducting Polymers*, 2nd ed., edited by T. Skotheim, R. E. Baumer, and J. Reynolds (Dekker, New York, 1998), pp. 85–122.
[6] S. R. Forrest, M. L. Kaplan, P. H. Schmidt, T. Venkatesan, and A. J. Lovinger, Appl. Phys. Lett. **4l**, 708 (1982).
[7] J. A. Osaheni, S. A. Jenekhe, A. Burns, G. Du, J. Joo, A. J. Epstein, and C. S. Wang, Macromolecules **25**, 5828 (1992).
[8] E. Tavenner, P. Meredith, G. Wood, M. T. Curry, and R. E. Giedd, Synth. Met. **145**, 183 (2004).
[9] Y. Q. Wang, R. E. Giedd, M. G. Moss, and J. Kaufmann, Nucl. Instrum. Methods Phys. Res. B **127/128**, 710 (1997).
[10] A. Tracz, J. Wosnitza, S. Barakat, J. Hagel, and H. Müller, Synth. Met. **120**, 849 (2001).
[11] See EPAPS Document No. E-APPLAB-89-002639 for methods and sample preparation. This document can be reached through a direct link in the online article's HTML reference section or via the EPAPS homepage (http://www.aip.org/pubservs/epaps.html).
[12] M. M. El-Bahay, M. E. El-Mossalamy, M. Madhy, and A. A. Bahgat, Phys. Status Solidi A **198**, 76 (2003).
[13] A. M. Goldman and N. Markovic, Phys. Today **51**, 39 (1998).